IN-SITU STUDY OF DEFORMATION AND INITIATION OF DUCTILE FRACTURE AT A NOTCH-ROOT

F. MOUSSY

Institut de Recherches de la Sidérurgie Française (IRSID)
185, Rue du Président Roosevelt, 78105 SAINT GERMAIN EN LAYE (France)

ABSTRACT

The search for a criterion of ductile fracture initiation at a notch-root is quite complex. Notch-root strains are often measured by means of indirect methods or on unloaded specimens. In addition, the existence of large strain gradients calls for very localized measurements. Finally, the definitions of initiation under these loading conditions are presently not fully satisfactory.

An original method developped by IRSID allowing the SEM observation of the notch-root deformations in situ and under load makes it possible to define the notion of initiation and the direct measurement of notch-root strains. With this method, the size of the gauge length can be as small as desired since it is not limited by anything but the heterogeneous nature of deformations at a microscopic scale.

Our observations show that strains have to be measured under load as unloading yields a 40 % reduction in longitudinal strain and a 30 % reduction in microcrack width.

JI and the longitudinal notch-root strain ε_1 are functions of both load deflection (d) and notch depth (a). Nevertheless we have shown that JI is directly related to ε_1 independently of the notch depth (a) as established theoretically by Rice.

JIc decreases slowly with increasing values of the notch depth (a).

To measure the critical local value of ε_1 at initiation one has to resort to a very small gauge length due to the deformation gradient. Deformations being heterogeneous at this microscopic scale, experimental measurements of local critical values of ε_1 at initiation display a large scatter. Therefore the use of such a local parameter appears to be hardly feasible.

KEYWORDS

Steel ; bend tests ; ductile fracture ; notch-root strains ; deformation mechanisms ; damage ; crack initiation ; fracture mechanics ; JIc.

INTRODUCTION

The search for a criterion of crack initiation at the root of a blunt notch under ductile fracture conditions is a delicate matter. Under these experimental conditions, initiation is difficult to define : several authors in fact give different definitions. Once initiation is defined, the determination of critical values (Klc, Jlc, ε_c, σ_c, etc.) is possble but there are various methods for measuring these values ; indirect methods exist, in particular for measuring notch-root strains but their validity is not always assured (Lequear and Lubahn, 1954). We have investigated specimens with a notch-root radius of 0.6 mm and different notch depths.

Notch-root deformation mechanisms are observed under load with the Scanning Electron Microscope (SEM). These observations yield a definition of initiation. Values for JI and longitudinal strain at the notch-root have been evaluated.

STRAIN MECHANISMS

Experimental Method

The steel composition is given in Table. I. This steel was given a treatment at 850°C for 30 mn followed by oil quenching, tempering at 550°C for 2 hours, and air cooling. Its mechanical properties are given in Table II.

TABLE I. Composition of Steel (% Weight).

C	Mn	Si	S	P	Ni	Cr	Mo	Cu	Al
0.295	0.54	0.31	0.005	0.019	2.02	1.86	0.39	0.04	0.01

TABLE II. Mechanical Properties at Room Temperature.

σ_{ys} (N.mm^{-2})	σ_{ut} (N.mm^{-2})	Elongation (%)	Reduction in area (%)
1076	1192	16	61

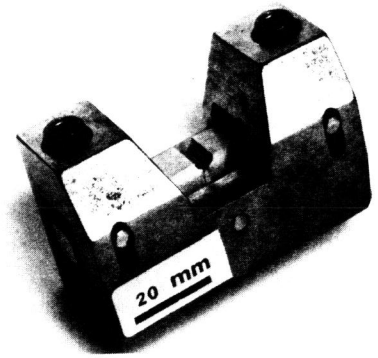

Fig. 1. Experimental device with a specimen under load.

In order to avoid unloading of the specimen and the strains associated to it, we have devised a system allowing the bending of the specimen and its observation under load with the SEM at high magnification. The system must be sufficiently small to enter the sample chamber of the SEM. The microscope used is an ISI Super II. The dimensions of its chamber allow the introduction of relatively voluminous objects. The bending device is shown in Fig. 1.

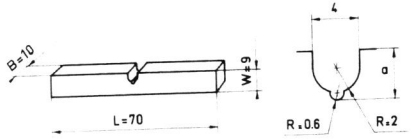

Fig. 2. Geometry and dimensions of the notch bend specimen (all specimen dimensions in mm).

The span length is 55 mm. A screw rotation reading device makes it possible to measure the load displacement with an accuracy better than 10 µm. The specimens used are shown in Fig. 2. The different values of a are 3, 4, 5 and 6 mm.

The surface condition of the notch root is of great importance with respect to the phenomena accompanying initiation : a rough-machined or poorly polished surface exhibits irregular behaviour (precocious cracking due to surface cold work). The notch surface is lapped and then polished to diamond 5 µm. The specimen is observed under the SEM before deformation and then taken from under the microscope. A first bending is carried out. The entire device is placed under the microscope and the notch root is again observed ; this operation is repeated for each strain level. A marking system makes it possible to follow the same areas during the different bending stages. Reference will be made below to the x_1, x_2 and x_3 axis related to the specimen as indicated in Fig. 3.

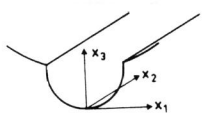

Fig. 3. Definition of the coordinate axis.

Description of Strain

At the beginning of bending, the strain appears to be uniform at the notch root but, under high magnification, it is very quickly noted that it is concentrated in narrow zones (a few µm wide) separating rigid blocks (from 10 to 30 µm approximately). The deformed zones, although winding, are mainly lined up along x_2 (Fig. 4-a and b).

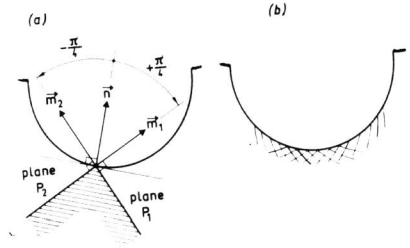

Fig. 5. Definition of the two types of primary shear planes P1 and P2.

They are formed by the emergence of intense shear planes, which we shall refer to as "primary shear". The "steps" thus created give rise to microcracks (a few µm long - Fig. 4-c and d) under a mode II solicitation. At this stage, the deformation and damaging of the metal are uniformly distributed over a zone which covers the bottom of the notch on both sides of the centerline over a width greater than 0.6 mm. These microcracks are all widened and extended simultaneously. The cracking plane contains the x2 axis and forms an angle of 45° with the notch root surface. It is thus possible to define two types of primary shear planes P_1 and P_2 (Fig. 5-a).

For cracks located far from the notch root and situated on the same side, there is only one type of plane. At the center, the two types P1 and P2 can exist together (Fig. 5-b) : in this central zone, two cracks can be aligned along x2 and have shear planes of two different types.

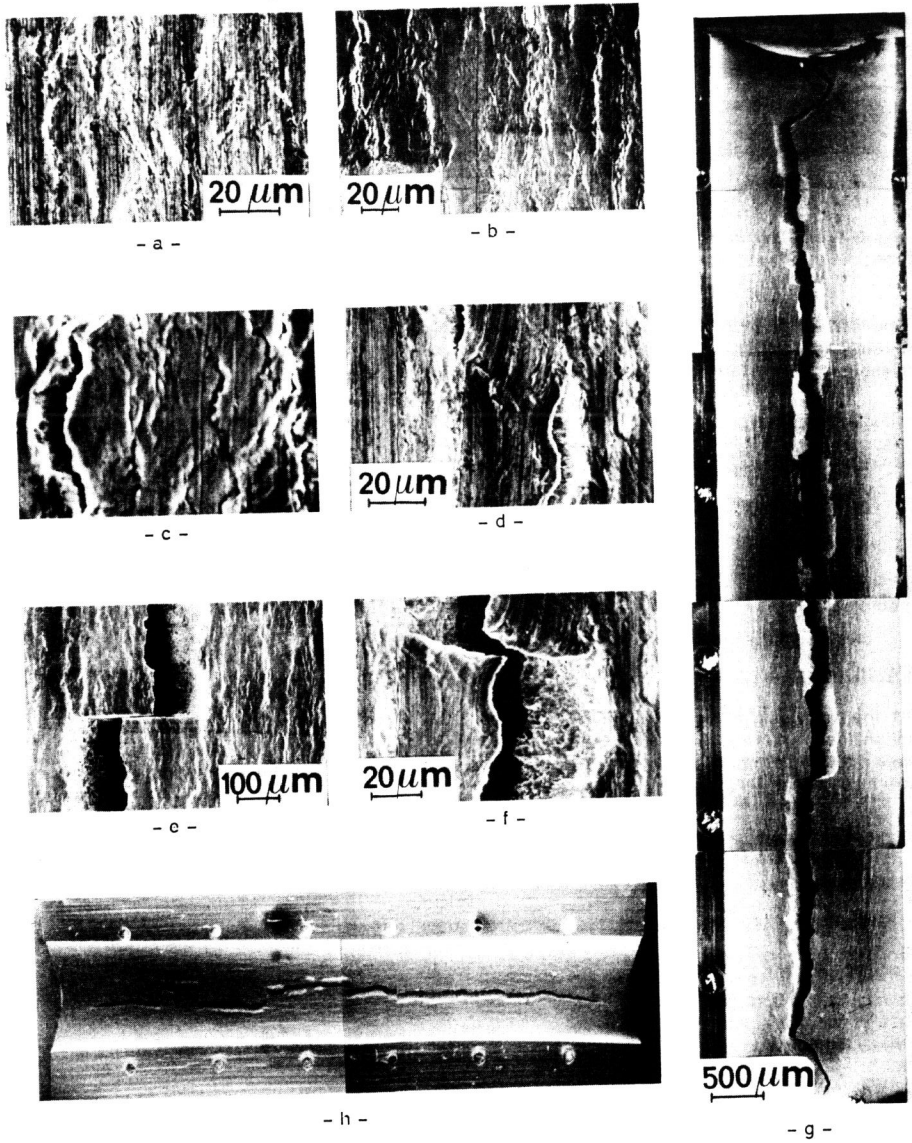

a - b : beginning of plastic deformation
c - d : "primary shear" (microcracks)
e - f : "secondary shear" (initiation of a macrocrack)
g - h : end of coalescence of surface microcracks
Nota : micrographs d and f are two deformation stages of the same field.

Fig. 4. Mechanisms of notch-root deformation in bending.

As the deformation progresses, certain microcracks are joined by an unique mechanism : shearing in a plane adjacent to $x_1\ x_3$, which we shall call "secondary shear" forming cracks subjected to mode III (Fig. 4-e and f). This shear allows the coalescence of non-colinear cracks (along x_2) or colinear cracks each having a different type of shear plane (P_1 and P_2). The macro-crack thus formed is then the only one to progress, the adjacent microcracks closing even partially under the effect of a relaxation of stresses. The advantage of observing bending strain mechanisms under load is apparent here. In the unloaded condition, certain phenomena are no longer observable ; we have shown cases of re-closing of crack edges by 30 % during unloading. This macrocrack progresses laterally along x_2 by the same mechanism (secondary shear) to finally occupy the entire specimen width (Fig. 4-g). The crack plane is then unique and parallel to $x_2\ x_3$ (mode I). In Fig. 4-h, the primary and secondary shear zones are clearly visible. At this stage of bending, the observation of strains is no longer possible because they are concentrated at the bottom of the deep crack and the surface of the notch is no longer deformed. Measures of ε_2 show that the central third of the specimen is in condition of plane strain. The surface of fracture is entirely ductile.

DEFINITION OF INITIATION

Initiation is difficult to define. The evolution of the deformation is often continuous. The definition chosen is thus arbitrary (critical size of flaws, holes or cracks for example). Initiation must be characterized by the appearance of a distinct event, a discontinuity in the mechanisms. Hancock and Mackenzie (1976), investigating the ductile fracture of notched tensile specimens, define initiation as the beginning of the coalescence of cavities formed around inclusions. For certain materials in which fracture is preceded very closely by instability, 7075 aluminium for example (Russo, Chakrabarti and Spretnak, 1977), initiation is identified with fracture. Lemaître and Chaboche (1978) state the problem more generally. They distinguish between two successive stages in the fracture of a metal : firstly, there is damage (creation of cavities around inclusions, microcracks) which leads to the initiation of a macrocrack ; secondly, there is the propagation of this macrocrack. The first stage is within the realm of damage, the second within that of fracture mechanics, the initiation being the border between the two. We have applied this concept to our metallographic observations. To define initiation, we consider the following to be necessary conditions :

- Appearance of a distinct event.
- Localization of strain leading rapidly to the creation of a single macrocrack.

If reference is made to the strain mechanisms described earlier, the first plastic stage (creation of steps), the appearance of microcracks (primary shear in planes P_1 and P_2) and the growth of these microcracks (independent of each other) are continuously evolving non-localized phenomena. They thus fall within the realm of damage. On the other hand, the appearance of secondary shear immediately leads to the creation of a macrocrack by rapid coalescence along x_2 of the microcracks and the localization of the strain by the propagation of the unique macrocrack in a plane parallel to $x_2\ x_3$. We will thus define initiation as the appearance of secondary shear. We made an optical micrograph in a plane $x_1\ x_3$ of a crack corresponding to this definition of initiation : owing to elastic deformation during the unloading phase (necessary for polishing), the two sides of the crack are in contact. The depth of this crack is about 60 µm (which is of the same order of magnitude as the primary shear width visible in Fig. 4-g and h).

When the strains are observed along x_1 on each side of the macrocrack, elastic deformation during unloading is noted with negative ε_1 values. This shows that the strain is localized as soon as the initiation thus defined occurs.

Although we have observed deformations in plane strain, we have tried to interpret our experimental observations with the help of the results of finite element method calculations in plane stress presented by Russo, Chakrabarti and Spretnak (1977) :

- The diffuse appearance of microcracks is a shear phenomenom taking place in mode II (primary shear). The controlling parameter must be the pure or maximum shear strain or the pure or maximum shear stress. The results of the calculations of Spretnak indicate that, in the central zone of the notch root and on the surface, the pure shear strain value is practically constant and then drops abruptly at a certain distance from the center of the notch. We explain so that the microcracks originate with equal probability over the entire notch root.

- The propagation of microcracks takes place along spiral lines forming an angle of 45° with the notch root surface. This is also in agreement with a pure shear strain criterion since the characteristic lines for the stresses are these logarithmic spirals (Hill, 1950).

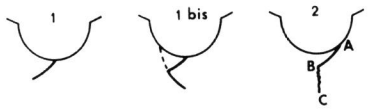

- When these microcracks progress, the mechanisms can be illustrated schematically by considering two particular cases (Fig. 6) :

Fig. 6. Different possible microcrack paths.

. A microcrack initiated at the notch root develops as it draws away from the axis of symmetry, i.e. from the most highly stressed zone. In fact, pure shear strain decreases on such a line when it is followed from the surface. The microcrack will thus stop (Case 1, Fig. 6) or will follow another characteristic line of pure shear strain ; the direction of the crack then changes by 90° (Case 1bis, Fig. 6).

. A microcrack initiated a certain distance from the center develops as it draws near the axis of symmetry and thus arrives within the most highly stressed zone. And precisely, pure shear strain increases when such a line is described from the surface. The progression can thus continue easily (Case 2, Fig. 6). In addition, while the microcrack progresses along the path AB, its length increases along x_2 as does that of the other microcracks. These defects will thus move together and those which are both near each other and the tip which is near the center line of the specimen (and hence highly stressed) will coalesce by secondary shear and the propagation of the macrocrack formed will continue along the path BC.

We have observed experimentally that the macrocrack was formed from surface microcracks located a certain distance from the notch center, but there is considerable scattering of values. The causes of the apparent localization of the initiation on the surface are perhaps not to be sought in the behaviour of the extreme surface but in that of the microcracks after a certain stage of development.

NOTCH ROOT STRAIN

The measurement of notch root strain is carried out under load using SEM micrographs. Notch dimensions are such that it is not possible to deposit a grid. In addition, the tracing of engraved markings disturbs the notch surface significantly (case of rough-machined or inadequately polished notches). It is the polishing streaks (width smaller than 1 µm) or inclusions which serve as markers. The precision is ± 1 %. The gauge length chosen must not be too large, because the strain gradients can lead to an underestimation of strains. It must not be too small either because, in a small scale, the strains are very heterogeneous (Fig. 4-a and b). Experience shows that a gauge length smaller than 150 µm is not realistic because it leads to very scattered results.

Our observations show, finally, that the use of large specimens and similitude laws to calculate strains on small specimens is valid only for the mechanics of continuous media and cannot be applied without precaution for the description of strain phenomena in the microscopic scale.

We have chosen an average measurement base between 200 and 300 µm.

RESULTS - DISCUSSION

The bending device for SEM observation makes it possible to :

- establish the ε_1 - load displacement curves ; we have often used the value of ε_1, at the notch root, noted ε_1^{max} ;

- determine the load displacement at initiation ;

- measure ε_{1c}, strain ε_1 at initiation over the range in which initiation takes place. ε_{1c} can be different from ε_1^{max}.

On the other hand, this device does not give access to load measurements. Bending tests were thus carried out in parallel on a tensile machine in order to obtain load-displacement curves.

Values of J_I and J_{Ic}

The values of J_I were calculated by two methods :

$$J_I = \frac{2U}{B(W-a)} \quad \text{and} \quad J_I = -\frac{1}{B}\left(\frac{\partial U}{\partial a}\right)_d$$

where U is the area under the load-displacement curve, d is the load displacement, the other values being defined in Fig. 2.

These two methods yield very similar results ; we have taken the average value.

Figure 7 shows the J_I - d curves for each notch depth. Knowing d at initiation, we calculate J_{Ic}.

J_{Ic} tends to decrease slightly as notch depth increases Fig. 8. A linear regression leads to :

$$J_{Ic} = -27\,a + 0.46 \quad \text{with } J_{Ic} \text{ in MPa.m and a in m} \qquad (1)$$

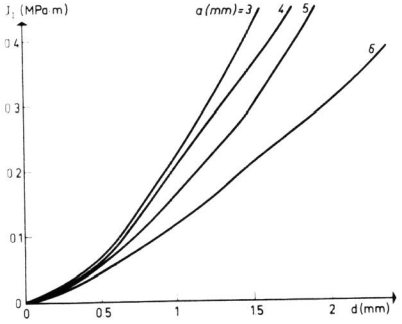

Fig. 7. J_I versus load displacement for different notch depths.

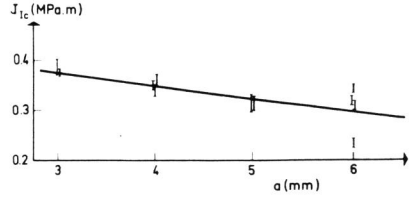

Fig. 8. J_{Ic} versus notch depth.

Relationship $J_I - \varepsilon_1^{max}$

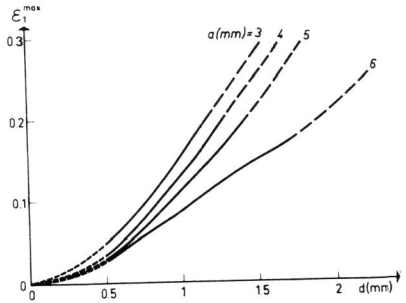

Fig. 9. Longitudinal notch-root strain versus load displacement for different notch depths.

We plotted in Fig. 9 the evolution of notch root strain along x1 noted ε_1^{max} as a function of d for different notch depths. Each curve is the average curve on several specimens, the scattering being small except in the very last stages. To each notch depth there corresponds a specific curve.

Rice (1968) showed that if the notch root is taken as the integration contour :

$$\varepsilon_1^{max} \sim \varepsilon_{1y} \left[\frac{(N+1/2).(N+3/2).\Gamma(N+1/2)}{\Gamma(1/2).\Gamma(N+1)} \; \frac{J_I}{\sigma_{1y}\, \varepsilon_{1y} rt} \right]^{1/(1+N)} \quad \text{with} \quad (2)$$

Γ = gamma function ; rt = notch root radius (constant)

σ_{1y} and ε_{1y} defined by $\sigma_1 = \varepsilon_{1y} \left(\frac{\varepsilon_1}{\varepsilon_{1y}}\right)^N$, the notch root behaviour law in the plastic domain.

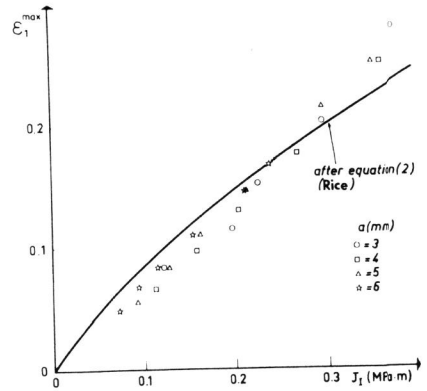

Fig. 10. Relationship between longitudinal notch-root strain and J_I for different load displacements and notch depths.

Knowing $J_I = f(d)$ and $\varepsilon_1^{max} = g(d)$, we deduce $\varepsilon_1^{max} = h(J_I)$. ε_1 and J_I are closely correlated and in a unique manner independent of the notch depth (Fig. 10).

The Rice equation (2) is shown in the same figure. To plot this curve, we used a specmen with a 3 mm notch depth. The notch root radius of curvature was determined under load with a contour projector. In the equation (2), the radius rt can vary with load displacement but, for a given bending stage, it is considered to be constant. For rt, we have taken the maximum value of the notch root radius of curvature i.e. at the center of notch; this zone provides the essential part of the Wdx1 contribution to the integral allowing the establishment of equation (2).

Agreement between theory and experiment is particularly remarkable. The experimental points nevertheless have a tendency to line up whereas the theoretical curve exhibits a concavity toward the J_I axis.

A linear regression carried out on the experimental points leads to :

$$\varepsilon_1^{max} = -3.2\ 10^{-3} + 0.7\ J_I \qquad J_I \text{ in (MPa.m)} \qquad (3)$$

with a correlation coefficient of 0.99.

We can consider that this linear regression goes through the origin of the axis.

Influence of notch depth on ε_{1c}

We conducted bending tests with the SEM following several fields per specimen. When initiation occurs on observed fields, it is possible to determine the local ε_{1c}. Figure 11 shows the results obtained for different notch depths. There is considerable experimental scattering of results. This is inherent in the method used : the crack often goes through the gauge length, and the crack width is not the same from one specimen to another. In addition, ε_{1c} results from a local measurement (gauge length of about 200 µm) and initiation probably takes place where the metal has an accentuated local weak point. Such phenomena, in the scale in which we have investigated them, have little chance of being reproductible. We have plotted, for information, the law $\varepsilon_{1c} = f(a)$ deduced from (1) and (3) considering that $\varepsilon_{1c} = \varepsilon_1^{max}$ at initiation.

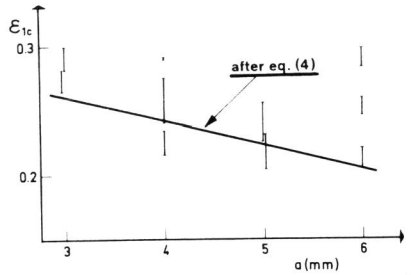

Fig. 11. Values of critical local longitudinal notch root strain at initiation for different notch depths.

$$\varepsilon_{1c} = 0.317 - 18.8\ a \qquad \text{with a in m.} \qquad (4)$$

CONCLUSION

The description of notch root strains under ductile fracture conditions has made it possible to distinguish two stages : gradual non-localized damage leading to the creation of a macrocrack, followed by the propagation of this macrocrack. Two types of shear are involved : primary (mode II) and secondary (mode III). The appearance of the latter shear characterizes initiation. With this definition, we have evaluated J_{Ic}, which decreases slightly with increasing notch depth.

Variations of J_I and notch-root strain ε_1 with load displacement depend upon the notch depth, but J_I and ε_1 are described by an unique relationship independant of notch depth. This relationship is in agreement with the theoretical formula established by J.R. Rice.

The direct measurements of local elongation at initiation yield scattered values. The experimental verification of local criteria is found to be very difficult and loses considerable meaning because it requires local observations on the microscopic level where deformation is heterogeneous.

ACKNOWLEDGEMENT

The author gratefully acknowledges. Cl. Quennevat for his assistance in the delicate experimental work.

REFERENCES

Hancock, J.W. and A.C. Mackenzie (1976) . J. Mech. Phys. Solids. Pergamon Press. Printed in Great Britain, vol. 24, p. 147-169.

Hill, R. (1950). The Mathematical Theory of Plasticity. Oxford at the Clarendon Press.

Lemaître, J. and J.L. Chaboche (1978) . Journal de Mécanique Appliquée, vol. 2, n° 3, p. 317-365.

Lequear, H.A. and J.D. Lubahn (1954) . Welding Research Council. Supplement of the Welding Journal, December, p. 585-588.

Rice, J.R. (1968) . J. Appl. Mech., June, p. 379-386.

Russo, V.J., A.K. Chakrabarti, and J.W. Spretnak (1977) . Met. Trans. A., vol. 8A, May, p. 729-740